Supplemental Online Content

Hanna GJ, Villa A, Nandi SP, et al. Nivolumab for patients with high-risk oral leukoplakia: a nonrandomized controlled trial. *JAMA Oncol.* Published online November 16, 2023. doi:10.1001/jamaoncol.2023.4853

This supplemental material has been provided by the authors to give readers additional information about their work.

eTable 1. Detailed Clinical and Pathologic Assessments of All Study Patients

ID	Prior diagnosis of early-stage oral cavity SCC	Pre-Treatment measurements / biopsies	Total pre-treatment composite score	Post-nivolumab measurements / biopsies	Total post-treatment composite score	% Change, Best Response	Change in Lesion size (S) or histology (H)
1	Yes	4.0 cm (L3), KUS (P0) 1.8 cm (L1), mild dysplasia (P1)	26.0	4.0 cm (L3), carcinoma 1.3 cm (L1), no re-biopsy	99.0*	--, PD	S, H
2	No	2.6 cm (L2), mild dysplasia (P1)	14.0	3.0 cm (L2), mild dysplasia (P1)	14.0	0, SD	--
3	No	3.5 cm (L3), mild dysplasia (P1) 2.0 cm (L2), KUS (P0) 5.0 cm (L3), KUS (P0)	58.0	3.5 cm (L3), mild dysplasia (P1) 1.1 cm (L1), mild dysplasia (P1) 4.5 cm (L3), KUS (P0)	52.0	-10.3, SD	S, H
4	No	4.6 cm (L3), mild dysplasia (P1)	24.0	4.0 cm (L3), mild dysplasia (P1)	24.0	0, SD	S
5	No	5.5 cm (L3), mild dysplasia (P1)	24.0	5.5 cm (L3), KUS (P0)	24.0	-8.3, SD	H
6	No	3.3 cm (L3), mild dysplasia (P1)	24.0	3.3 cm (L3), mild dysplasia (P1)	24.0	0, SD	--
7	No	2.0 cm (L2), moderate dysplasia (P2)	16.0	1.1 cm (L1), mild dysplasia (P1)	4.0	-75.0, PR	S, H
8	Yes	1.5 cm (L1), mild dysplasia (P1)	4.0	0.4 cm (L1), mild dysplasia (P1)	4.0	0, SD	S
9	No	1.9 cm (L1), mild dysplasia (P1) 1.1 cm (L1), KUS (P0)	6.0	1.2 cm (L1), KUS (P0) 1.8 cm (L1), KUS (P0)	6.0	0, SD	S, H
10	No	1.7 cm (L1), KUS (P0) 1.5 cm (L1), KUS (P0) 0.5 cm (L1), moderate dysplasia (P2)	10.0	1.6 cm (L1), moderate dysplasia (P2) 0.9 cm (L1), KUS (P0) 0.8 cm (L1), mild dysplasia (P1)	12.0	+20.0, PD	S, H
11	No	2.0 cm (L2), KUS (P0) 2.1 cm (L2), mild dysplasia (P1) 4.0 cm (L3), mild dysplasia (P1)	50.0	1.0 cm (L1), mild dysplasia (P1) 2.3 cm (L2), KUS (P0) 2.0 cm (L2), KUS (P0)	28.0	-44.0, PR	S, H
12	No	1.5 cm (L1), mild dysplasia (P1)	4.0	0.4 cm (L1), mild dysplasia (P1)	4.0	0, SD	S
13	No	2.1 cm (L2), mild dysplasia (P1)	14.0	1.2 cm (L1), KUS (P0)	2.0	-85.7, PR	S, H
14	Yes	3.6 cm (L3), mild dysplasia (P1)	24.0	4.2 cm (L3), carcinoma	99.0	--, PD	S, H
15	No	2.5 cm (L2), mild dysplasia (P1) 0.4 cm (L1), mild dysplasia (P1)	18.0	2.5 cm (L2), mild dysplasia (P1) 0 cm (L0)	14.0	-22.2, SD	S
16	No	3.0 cm (L2), moderate dysplasia (P2)	16.0	1.2 cm (L2), mild dysplasia (P1)	4.0	-75.0, PR	S, H
17	No	2.5 cm (L2), mild dysplasia (P1)	14.0	2.5 cm (L2), mild dysplasia (P1)	14.0	0, SD	--
18	No	2.3 cm (L2), mild dysplasia (P1)	14.0	1.5 cm (L1), mild dysplasia (P1)	4.0	-71.4, PR	S
19	No	3.0 cm (L2), moderate dysplasia (P2)	16.0	0.4 cm (L1), mild dysplasia (P1)	4.0	-75.0, PR	S, H
20	Yes	0.5 cm (L1), mild dysplasia (P1) 4.0 cm (L3), moderate dysplasia (P2)	30.0	1.4 cm (L1), KUS (P0) 1.8 cm (L1), mild dysplasia (P1)	4.0	-86.7, CR	S, H
21	Yes	1.5 cm (L1), moderate dysplasia (P2) 1.0 cm (L1), moderate dysplasia (P2)	26.0	4.0 cm (L3), carcinoma 1.0 cm (L1), no re-biopsy	99.0	--, PD	S, H
22	No	1.5 cm (L1), mild dysplasia (P1)	4.0	0.3 cm (L1), KUS (P0)	2.0	-50.0, PR	S, H
23	Yes	4.5 cm (L3), moderate dysplasia (P2)	26.0	Patient refused re-biopsy	--	--	--
24	No	1.7 cm (L1), mild dysplasia (P1) 4.5 cm (L3), mild dysplasia (P1)	28.0	0 cm (L0) 0.2 cm (L1), moderate dysplasia (P2)	6.0	-78.6, PR	S, H
25	No	2.3 cm (L2), moderate dysplasia (P2)	16.0	2.0 cm (L2), moderate dysplasia (P2)	16.0	0, SD	S

26	Yes	4.5 cm (L3), mild dysplasia (P1) 3.2 cm (L3), mild dysplasia (P1)	24.0	4.5 cm (L3), mild dysplasia (P1) 3.5 cm (L3), mild dysplasia (P1)	24.0	0, SD	S
27	No	1.5 cm (L1), mild dysplasia (P1)	4.0	1.5 cm (L1), mild dysplasia (P1)	4.0	0, SD	--
28	No	2.3 cm (L2), mild dysplasia (P1)	14.0	0.1 cm (L1), KUS (P0)	2.0	-85.7, CR	S, H
29	No	3.4 cm (L3), mild dysplasia (P1)	24.0	2.0 cm (L2), mild dysplasia (P1)	14.0	-41.7, PR	S
30	Yes	2.3 cm (L2), severe dysplasia (P3)	18.0	2.5 cm (L2), severe dysplasia (P3)	18.0	0, SD	S
31	No	1.6 cm (L1), mild dysplasia (P1)	4.0	0.1 cm (L1), KUS (P0)	2.0	-50.0, PR	S, H
32	No	1.7 cm (L1), mild dysplasia (P1)	4.0	1.5 cm (L1), mild dysplasia (P1)	4.0	0, SD	S
33	No	2.0 cm (L2), mild dysplasia (P1)	14.0	2.0 cm (L2), KUS (P0)	12.0	-14.3, SD	H

SCC=squamous cell carcinoma, KUS=keratosis of undetermined significance without dysplasia, also referred to hyperkeratosis, not reactive; CR=complete response, PR=partial response, SD=stable disease, PD=progressive disease or carcinoma; (*) scores of 99 implies development of carcinoma at re-biopsy.

eTable 2. Association Between Clinical and Pathologic Parameters and Cancer-Free Survival

Variable	Total (N=33)[A]	
	HR	[95% CI]
Gender (male vs. female)	1.34	0.36-5.06
Age at registration (continuous)[B]	1.08	0.99-1.18
Smoking history (yes vs. no)	0.55	0.15-2.05
Primary leukoplakia subsite (tongue vs. other sites)	3.64	0.76-17.54
TMB per megabase (continuous)[B]	1.15	0.73-1.79
PD-L1 CPS (continuous)[B]	1.01	0.98-1.03
PD-L1 CPS (≥20 vs. <20)	1.92	0.46-8.04
History of prior oral squamous cell carcinoma (yes vs. no)	13.53	3.30-55.52
Pre-treatment or (baseline) composite score (continuous)[B]	1.04	1.00-1.08

[A] except TMB where N=20; [B] for every increase in age at registration the risk of CFS event increases by 8%; for every increase in TMB per megabase, the risk of CFS event increases by 15%; for every increase in CPS, the risk of CFS event increases by 1% and for every increase in pre-treatment composite score, the risk of CFS event increases by 4%; HR=hazard ratio (univariate estimates shown), CI=confidence interval, CPS=combined positive score. Univariate Cox proportional hazard modeling (HR>1: higher risk of CFS event).

eTable 3. Adverse Events Potentially Attributable to Nivolumab (N=33)

Toxicity	Number of patients (%)	Grade 1 or 2	Grade 3	Grade 4
Fatigue	18 (55)	17	1	0
Oral pain	11 (33)	11	0	0
Diarrhea	9 (27)	8	1	0
Itching	7 (21)	7	0	0
Dyspnea	7 (21)	7	0	0
Headache	7 (21)	7	0	0
Skin rash	6 (18)	5	1	0
Hypothyroidism	6 (18)	6	0	0
Elevated AST	6 (18)	5	0	1
Elevated ALT	6 (18)	5	1	0
Hypophosphatemia	4 (12)	4	0	0
GI disorder other	4 (12)	4	0	0
Cough	4 (12)	4	0	0
Abdominal pain	4 (12)	4	0	0
Arthralgia	4 (12)	4	0	0
Hyperthyroidism	3 (9)	3	0	0
Chest pain	2 (6)	1	1	0
Troponin elevation	1 (3)	0	1	0
Hyponatremia	1 (3)	0	0	1
Hyperglycemia	1 (3)	0	1	0
Gastritis	1 (3)	0	1	0
Endocrine disorder other	1 (3)	0	1	0
Elevated total bilirubin	1 (3)	0	1	0
Atrial fibrillation	1 (3)	0	1	0
Worst degree[A]	--	**25**	**6**	**1**

[A] this row adds to N=32 because one patient had no post-baseline adverse events. Frequencies are shown above (%). Note: no grade 5 AEs were reported. Only grade 1-2 events reported in >10% of patients are listed, and all grade 3-4 events are listed. Abbreviations: AST=Aspartate aminotransferase, ALT=Alanine aminotransferase, GI=gastrointestinal.

eTable 4. Clinical and Pathologic Predictors of Response*

Covariate	Total ($N = 33$)[A]	
	OR	[95% CI]
Gender (male vs. female)	0.45	0.10-1.92
Age at registration (continuous)[B]	0.99	0.92-1.06
Smoking history (yes vs. no)	1.10	0.26-4.64
Primary leukoplakia subsite (tongue vs. other sites)	1.10	0.26-4.64
TMB per megabase (continuous)[B]	0.83	0.44-1.41
PD-L1 CPS (continuous)[B]	1.03	1.00-1.06
PD-L1 CPS (≥20 vs. <20)	4.29	0.83-25.94

[A] except for TMB where N=20; [B] for every increase in age at registration the odds of being CR/PR decreased by 1%, for every increase in TMB per megabase; the odds of being in CR/PR decrease by 17.1%, and for every increase in CPS; the odds of being in CR/PR increase by 2.8%; OR=odds ratio (univariate estimates shown), CI=confidence interval, CPS=combined positive score; Univariate logistic regression analysis (OR>1: higher probability of response).

*Categorizing response with an already small sample size reduces power. Linear regression (with post-treatment composite score as the outcome) was used to assess for variability in the pre-treatment (baseline) composite score. First, with pre-treatment PD-L1 CPS alone as primary predictor in the linear regression model: for every 1 unit increase in PD-L1 CPS, post-treatment composite score decreases by 0.06 [post treatment composite score = 13.12-0.06*pre-treatment PD-L1 CPS]; when PD-L1 CPS as the primary clinical predictor adjusted for pre-treatment composite score (all variables are continuous), results are similar: for every 1 unit increase in pre-treatment PD-L1 CPS, post-treatment composite score decreases by 0.11 [post-treatment composite score = 1.05+0.73* pre-treatment composite score-0.11*pre-treatment PD-L1 CPS].

eFigure 1. Measurement of Effect and Response Assessment

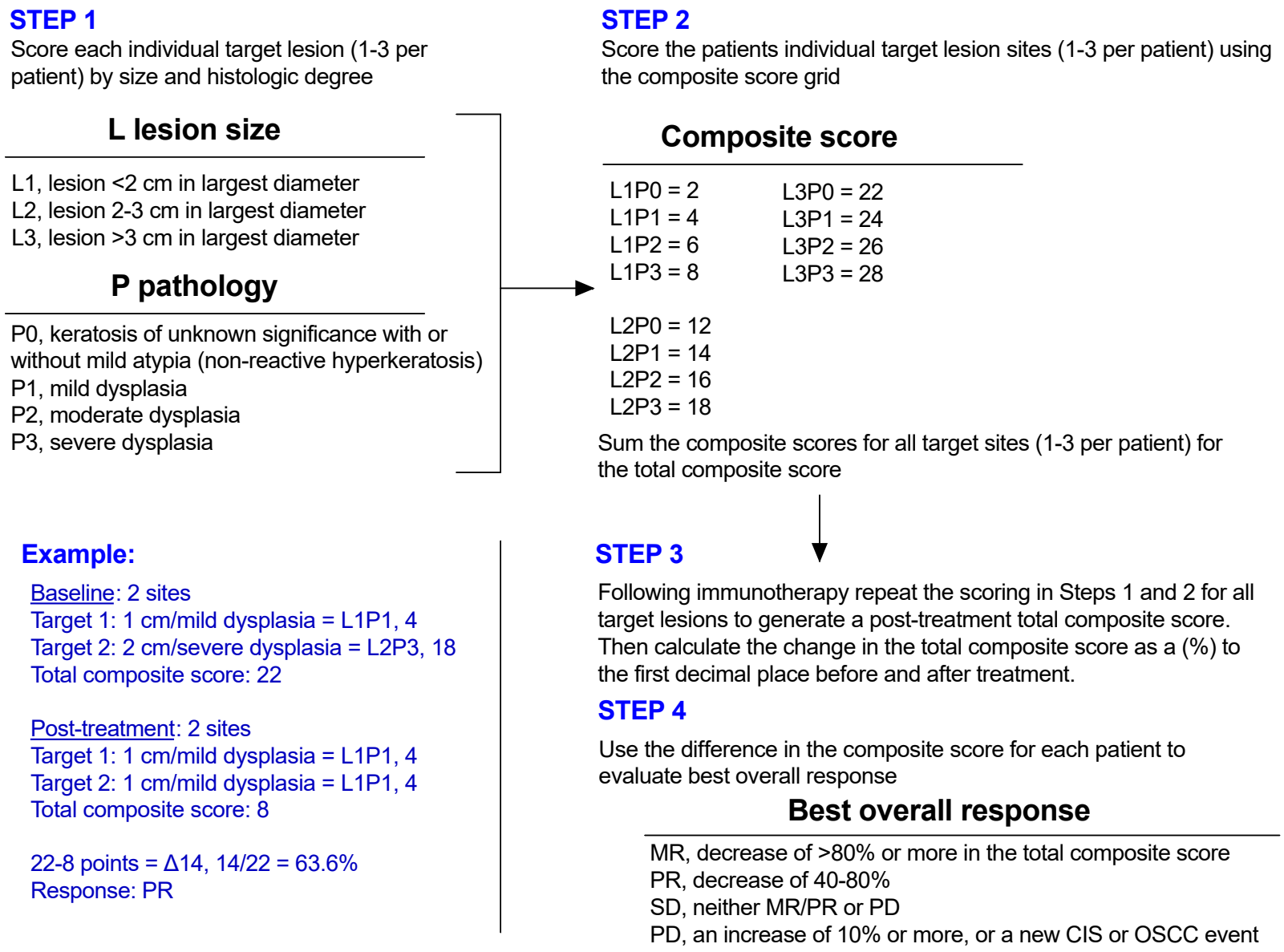

eFigure 2. Immunologic Correlates of Response and Survival

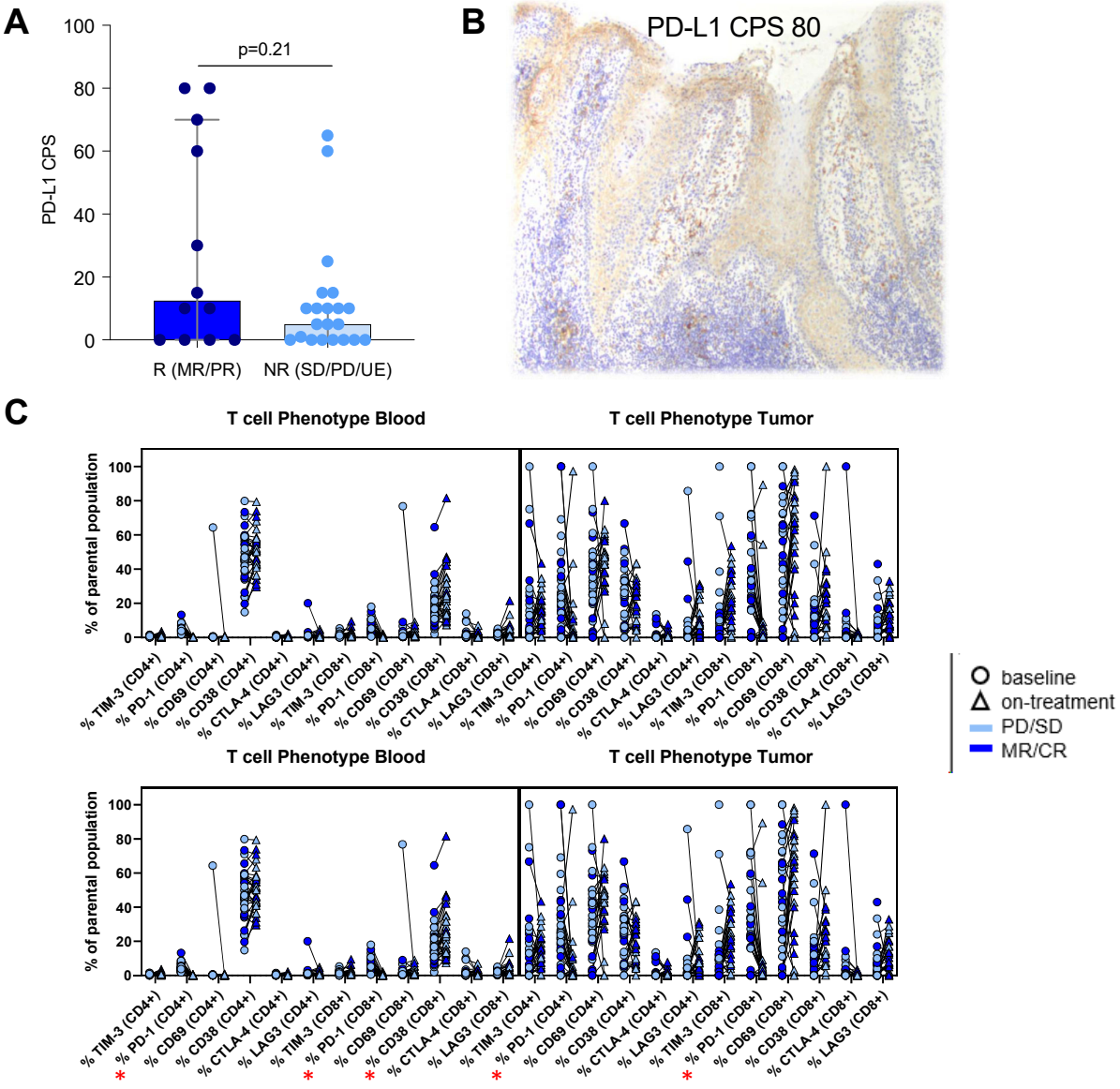

eMethods

PD-L1 IHC

Immunohistochemical quantitative analysis for PD-L1 on baseline epithelial dysplasia tissue samples was obtained using in-house staining (E1L3N clone, Cell Signaling Technology) and reported as a combined positive score (CPS) (range: 0-100) as scored by an expert head and neck pathologist [VJ, KW] blinded to outcome data. CPS reflected scoring on intralesional epithelial cells of leukoplakia and associated inflammatory cells.

Tissue and peripheral blood immunoprofiling

Fresh tissues were enzymatically disaggregated in RPMI (Life Technologies) +10% FBS (HyClone), 100 U/ml collagenase type IV (Life Technologies), and 50 μg/ml DNase I (Roche) at 37°C for 45 minutes and strained through a 40μm filter. The PBMC layers from blood samples were isolated after centrifugation for 10min at 1000g. Red blood cells were removed from samples using red blood cell lysis buffer (Biolegend). Cells were incubated with the Live/Dead Zombie NIR (Biolegend) for 5 min in the dark at room temperature. Fc receptors were blocked prior to surface antibody staining using mouse FcR Blocking Reagent (Biolegend). Cells were stained for 15min on ice in the dark and washed 2x with PBS + 2% FBS. Cells were analyzed on a BD LSRFortessa with FACSDiva software (BD Biosciences). Data were analyzed using FlowJo software version 10.7.2. Antibodies were specific for the following human markers: CD69 (FN50), CD38 (HIT2), LAG-3 (11C3C65), TIM-3 (F38-2E2), CD3 (UCHT1), PD-1 (EH12.1), CD45RA (HI100), CTLA-4 (BNI3), CD45 (HI30), CD4 (RPA-T4), CD16 (3G8), CD33 (WM53), PD-L2 (24F.10C12), CD56 (B159), PD-L1 (29E.2A3), CD15 (W6D3), CD31

(WM59), CD19 (HIB19), CD14 (M5E2) from Biolegend; CCR7 (150503), HLA-DR (G46-6) and CD8 (RPA-T8) from Thermo Fisher Scientific.

Tissue and peripheral blood whole-exome sequencing (WES)

Initial processing of pre-treatment epithelial dysplastic tissue samples was performed at the UCSD Biorepository & Tissue Technology Shared Resource Center. Briefly, paraffin was removed from formalin-fixed, paraffin-embedded (FFPE) tissue sections and cores using CitriSolv (Fisher Scientific) followed by ethanol washes, and then tissue was lysed overnight at 56°C. Samples were then incubated at 90°C to remove DNA crosslinks, and extraction was performed using Qiagen's QIAamp DNA FFPE Tissue Kit. DNA from matching patient peripheral blood mononuclear cells (PBMCs) were extracted using the ALLPREP DNA/RNA Mini Kit. Both FFPE tissue and PBMC DNA were sent to Novogene (Sacramento, CA). DNA whole-exome sequencing library preparation was performed using the IDT xGen Exome Panel v2 kit following the manufacturer's recommendations. Qualified libraries were sequenced on an Illumina platform according to effective concentration and data volume. For FFPE tissue samples, the effective coverage of sequencing was 200X and for PBMC match-normal samples the effective coverage was 100X.

WES DNA assembly and quality control

Post-sequencing analysis was performed within Triton Shared Compute Cluster (TSCC) at the University of California, San Diego. Briefly, quality assurance of the raw FASTQ files were evaluated using FastQC and Mosdepth [1, 2]. Raw sequence reads were aligned to the human reference genome GRCh38. The aligned reads were marked duplicated using MarkDuplicates

(Picard) – GATK [3]. Concordance between tumor and matched normal samples were evaluated using Conpair [4] and only samples with >99.5% concordance were taken forward for subsequent analysis.

WES somatic alteration identification and annotation

EnsembleVariantCallingPipeline (EVC) was used to call single nucleotide variants (SNV) and short INDELS. EVC implements the SNV and INDEL variant calling from four variant callers (Mutect2, Strelka2, Varscan2, MuSE) and only passed mutations called with any two variant callers were considered true mutations [3, 5-7]. Following annotation of each variant with Ensembl Variant Effect Predictor (VEP, version 106), somatic mutations were taken forward for amino acid change detection [8]. Oncoplot was generated using Maftools [9]. Possible involvement of driver gene mutations was identified with IntOGen [10]. Copy number alteration detection was performed with ASCAT (v3.1) [11] and focal somatic copy number alterations were detected with GISTIC2.0 [12]. Fisher exact tests were performed within R statistical language [13]. Mutational profile and signature analysis were performed with SigProfiler bioinformatic tools developed within the Alexandrov lab [14, 15] at UC San Diego. Plotting of figures was performed with Adobe Illustrator and Prism.

eReferences

1. http://www.bioinformatics.babraham.ac.uk/projects/fastqc.
2. Pedersen BS, Q.A., Mosdepth: quick coverage calculation for genomes and exomes. Bioinformatics, 2018. 34(5): p. 867-8.
3. McKenna A, H.M., Banks E, Sivachenko A, Cibulskis K, Kernytsky A, Garimella K, Altshuler D, Gabriel S, Daly M, DePristo MA, The Genome Analysis Toolkit: a MapReduce framework for analyzing next-generation DNA sequencing data. Genome Res, 2010. 20(9): p. 1297-303.
4. Bergmann EA, C.B., Arora K, Vacic V, Zody MC, Conpair: concordance and contamination estimator for matched tumor-normal pairs. Bioinformatics, 2016. 32(20): p. 3196-8.
5. Fan Y, X.L., Hughes DS, Zhang J, Zhang J, Futreal PA, Wheeler DA, Wang W, MuSE: accounting for tumor heterogeneity using a sample-specific error model improves sensitivity and specificity in mutation calling from sequencing data. Genome Biol, 2016. 17(1): p. 178.
6. Kim S, S.K., Halpern AL, Bekritsky MA, Noh E, Källberg M, Chen X, Kim Y, Beyter D, Krusche P, Saunders CT, Strelka2: fast and accurate calling of germline and somatic variants. Nat Methods, 2018. 15(8): p. 591-4.
7. Koboldt DC, Z.Q., Larson DE, Shen D, McLellan MD, Lin L, Miller CA, Mardis ER, Ding L, Wilson RK, VarScan 2: somatic mutation and copy number alteration discovery in cancer by exome sequencing. Genome Res, 2012. 22(3): p. 568-76.
8. McLaren W, G.L., Hunt SE, Riat HS, Ritchie GR, Thormann A, Flicek P, Cunningham F, The Ensembl Variant Effect Predictor. Genome Biol, 2016. 17(1): p. 122.
9. Mayakonda A, L.D., Assenov Y, Plass C, Koeffler HP, Maftools: efficient and comprehensive analysis of somatic variants in cancer. Genome Res, 2018. 28(11): p. 1747-56.
10. Gonzalez-Perez A, P.-L.C., Deu-Pons J, Tamborero D, Schroeder MP, Jene-Sanz A, Santos A, Lopez-Bigas N, IntOGen-mutations identifies cancer drivers across tumor types. Nat Methods, 2013. 10(11): p. 1081-2.
11. Van Loo P, N.S., Lingjærde OC, Russnes HG, Rye IH, Sun W, Weigman VJ, Marynen P, Zetterberg A, Naume B, Perou CM, Børresen-Dale AL, Kristensen VN, Allele-specific copy number analysis of tumors. Proc Natl Acad Sci USA, 2010. 107(39): p. 16910-5.
12. Mermel CH, S.S., Hill B, Meyerson ML, Beroukhim R, Getz G, GISTIC2.0 facilitates sensitive and confident localization of the targets of focal somatic copy-number alteration in human cancers. Genome Biol, 2011. 12(4): p. R41.
13. R Core Team (2013) R: A Language and Environment for Statistical Computing. R Foundation for Statistical Computing, V. and http://www.R-project.org/.
14. Bergstrom EN, H.M., Mahto U, Barnes M, Stratton MR, Rozen SG, Alexandrov LB, SigProfilerMatrixGenerator: a tool for visualizing and exploring patterns of small mutational events. BMC Genomics, 2019. 20(1): p. 685.
15. S M Ashiqul Islam, M.D.-G., Yang Wu, Mark Barnes, Raviteja Vangara, Erik N Bergstrom, Yudou He, Mike Vella, Jingwei Wang, Jon W Teague, Peter Clapham, Sarah Moody, Sergey Senkin, Yun Rose Li, Laura Riva, Tongwu Zhang, Andreas J Gruber, Christopher D Steele, Burçak Otlu, Azhar Khandekar, Ammal Abbasi, Laura Humphreys, Natalia Syulyukina, Samuel W Brady, Boian S Alexandrov, Nischalan Pillay, Jinghui Zhang, David J Adams, Iñigo Martincorena, David C Wedge, Maria Teresa Landi, Paul Brennan, Michael R Stratton, Steven G Rozen, Ludmil B Alexandrov, Uncovering novel mutational signatures by de novo extraction with SigProfilerExtractor. bioRxiv, 2020. https://doi.org/10.1101/2020.12.13.422570.